Research Article | Vol. 8, No. 9 | 1 Sep 2017 | BIOMEDICAL OPTICS EXPRESS 4172
Biomedical Optics EXPRESS

Crystalline lens paradoxes revisited: significance of age-related restructuring of the GRIN

CONOR J. SHEIL [1,2] AND ALEXANDER V. GONCHAROV [1,3]

[1]*Applied Optics Group, School of Physics, National University of Ireland, Galway, University Road, Galway, Ireland*
[2]*conor.sheil@nuigalway.ie*
[3]*alexander.goncharov@nuigalway.ie*

Abstract: The accommodating volume-constant age-dependent optical (AVOCADO) model of the crystalline lens is used to explore the age-related changes in ocular power and spherical aberration. The additional parameter *m* in the GRIN lens model allows decoupling of the axial and radial GRIN profiles, and is used to stabilise the age-related change in ocular power. Data for age-related changes in ocular geometry and lens parameter *P* in the axial GRIN profile were taken from published experimental data. In our age-dependent eye model, the ocular refractive power shows behaviour similar to the previously unexplained "lens paradox". Furthermore, ocular spherical aberration agrees with the data average, in contrast to the proposed "spherical aberration paradox". The additional flexibility afforded by parameter *m*, which controls the ratio of the axial and radial GRIN profile exponents, has allowed us to study the restructuring of the lens GRIN medium with age, resulting in a new interpretation of the origin of the power and spherical aberration paradoxes. Our findings also contradict the conceptual idea that the ageing eye is similar to the accommodating eye.

OCIS codes: (080.2710) Inhomogeneous optical media; (330.4460) Ophthalmic optics and devices; (330.5370) Physiological optics; (330.7323) Visual optics, aging changes; (330.7326) Visual optics, modelling.

References and links

1. R. Navarro, "The optical design of the human eye: a critical review," Journal of Optometry **2**, 3–18 (2009).
2. C. J. Sheil and A. V. Goncharov, "Accommodating volume-constant age-dependent optical (AVOCADO) model of the crystalline GRIN lens," Biomed. Opt. Express **7**, 1985–1999 (2016).
3. M. Bahrami and A. V. Goncharov, "Geometry-invariant gradient refractive index lens: analytical ray tracing," J. Biomed. Opt. **17**, 055001 (2012).
4. A. Sharma, D. V. Kumar, and A. K. Ghatak, "Tracing rays through graded-index media: a new method," Appl. Opt. **21**, 984–987 (1982).
5. E. Martinez-Enriquez, P. Pérez-Merino, M. Velasco-Ocana, and S. Marcos, "Oct-based full crystalline lens shape change during accommodation in vivo," Biomed. Opt. Express **8**, 918–933 (2017).
6. C. J. Sheil, M. Bahrami, and A. V. Goncharov, "An analytical method for predicting the geometrical and optical properties of the human lens under accommodation," Biomed. Opt. Express **5**, 1649–1663 (2014).
7. R. Navarro and N. López-Gil, "Impact of internal curvature gradient on the power and accommodation of the crystalline lens," Optica **4**, 334–340 (2017).
8. N. Brown, "The change in lens curvature with age," Exp. Eye Res. **19**, 175–183 (1974).
9. J. F. Koretz and G. H. Handelman, "The 'lens paradox' and image formation in accommodating human eyes," in "The lens: transparency and cataract: Proceedings of the EURAGE/BBS Symposium," G. Duncan, ed. (Eurage, 1986), pp. 57–64.
10. B. A. Moffat, D. A. Atchison, and J. M. Pope, "Explanation of the lens paradox," Optom. Vis. Sci. **79**, 148–150 (2002).
11. T. Grosvenor, "Changes in spherical refraction during the adult years," in "Refractive anomalies. Research and clinical applications," T. Grosvenor and M. Flom, eds. (Butterworth-Heinemann, Boston, 1991), pp. 131–145.
12. D. A. Atchison, E. L. Markwell, S. Kasthurirangan, J. M. Pope, G. Smith, and P. G. Swann, "Age-related changes in optical and biometric characteristics of emmetropic eyes," J. Vis. **8**, 1–20 (2008).
13. K. Attebo, R. Q. Ivers, and P. Mitchell, "Refractive errors in an older population: The blue mountains eye study," Ophthalmology **106**, 1066–1072 (1999).
14. H. Saunders, "Age-dependence of human refractive errors," Ophthalmic Physiol. Opt. **1**, 159–174 (1981).

#293354 https://doi.org/10.1364/BOE.8.004172
Journal © 2017 Received 21 Apr 2017; revised 26 Jul 2017; accepted 26 Jul 2017; published 22 Aug 2017

Biomedical Optics EXPRESS

15. H. Saunders, "A longitudinal study of the age-dependence of human ocular refraction—i. age-dependent changes in the equivalent sphere," Ophthalmic Physiol. Opt. **6**, 39–46 (1986).
16. C. Shufelt, S. Fraser-Bell, M. Ying-Lai, M. Torres, R. Varma, and the Los Angeles Latino Eye Study Group, "Refractive error, ocular biometry, and lens opalescence in an adult population: The Los Angeles latino eye study," Invest. Ophthalmol. Vis. Sci. **46**, 4450–4460 (2005).
17. Q. Wang, B. E. Klein, R. Klein, and S. E. Moss, "Refractive status in the beaver dam eye study." Invest. Ophthalmol. Vis. Sci. **35**, 4344–4347 (1994).
18. S.-Y. Wu, B. Nemesure, M. C. Leske, and for the Barbados Eye Study Group, "Refractive errors in a black adult population: The Barbados eye study," Invest. Ophthalmol. Vis. Sci. **40**, 2179–2184 (1999).
19. N. A. Brown and A. R. Hill, "Cataract: the relation between myopia and cataract morphology." Br. J. Ophthalmol. **71**, 405–414 (1987).
20. R. Lim, P. Mitchell, and R. G. Cumming, "Refractive associations with cataract: the blue mountains eye study," Invest. Ophthalmol. Vis. Sci. **40**, 3021 (1999).
21. C. Younan, P. Mitchell, R. G. Cumming, E. Rochtchina, and J. J. Wang, "Myopia and incident cataract and cataract surgery: The blue mountains eye study," Invest. Ophthalmol. Vis. Sci. **43**, 3625 (2002).
22. D. A. Atchison and G. Smith, *Optics of the Human Eye* (Butterworth-Heinemann, 2000).
23. J. Tabernero, E. Berrio, and P. Artal, "Modeling the mechanism of compensation of aberrations in the human eye for accommodation and aging," J. Opt. Soc. Am. A **28**, 1889–1895 (2011).
24. Y. Le Grand and S. G. El Hage, *Physiological Optics* (Springer-Verlag, 1980).
25. M. Dubbelman and G. van der Heijde, "The shape of the aging human lens: curvature, equivalent refractive index and the lens paradox," Vision Res. **41**, 1867–1877 (2001).
26. M. Dubbelman, G. van der Heijde, and H. Weeber, "The thickness of the aging human lens obtained from corrected scheimpflug images." Optom. Vis. Sci. **78**, 411–416 (2001).
27. T. Oshika, S. D. Klyce, R. A. Applegate, and H. C. Howland, "Changes in corneal wavefront aberrations with aging," Invest. Ophthalmol. Vis. Sci. **40**, 1351–1355 (1999).
28. A. Guirao, M. Redondo, and P. Artal, "Optical aberrations of the human cornea as a function of age," J. Opt. Soc. Am. A **17**, 1697–1702 (2000).
29. R. Navarro, "Adaptive model of the aging emmetropic eye and its changes with accommodation," J. Vis. **14**, 21 (2014).
30. I. Escudero-Sanz and R. Navarro, "Off-axis aberrations of a wide-angle schematic eye model," J. Opt. Soc. Am. A **16**, 1881–1891 (1999).
31. R. Navarro, F. Palos, and L. González, "Adaptive model of the gradient index of the human lens. I. formulation and model of aging ex vivo lenses," J. Opt. Soc. Am. A **24**, 2175–2185 (2007).
32. L. N. Thibos, X. Hong, A. Bradley, and R. A. Applegate, "Accuracy and precision of objective refraction from wavefront aberrations," J. Vis. **4**, 9 (2004).
33. T. O. Salmon and C. van de Pol, "Normal-eye zernike coefficients and root-mean-square wavefront errors," J. Cataract. Refract. Surg. **32**, 2064–2074 (2006).
34. C. E. Campbell, "Nested shell optical model of the lens of the human eye," J. Opt. Soc. Am. A **27**, 2432–2441 (2010).
35. J. F. Koretz, C. A. Cook, and P. L. Kaufman, "Accommodation and presbyopia in the human eye. changes in the anterior segment and crystalline lens with focus." Investigative Ophthalmol. Vis. Sci. **38**, 569–578 (1997).
36. J. Tabernero, A. Benito, E. Alcón, and P. Artal, "Mechanism of compensation of aberrations in the human eye," J. Opt. Soc. Am. A **24**, 3274–3283 (2007).

1. Introduction

The human eye has been studied extensively over the past century or so. More advanced measurements are becoming available, yet we still do not fully understand the structure of the human lens. With more advanced data, we require more realistic models for their reconciliation [1]. The usefulness of models lies in their ability to be optimised to provide results for different scenarios that cannot be observed experimentally. For example, they can provide information on the aged eye, of which measurements cannot be made due to the presence of severe cataract.

In traditional reverse optical engineering, the optical system is optimised to produce the required output. In the case of the human eye, much the same procedure is followed, but the human lens is not a simple homogeneous element; rather, the lens consists of a gradient index (GRIN) medium. We therefore see that optimisation of the lens parameters becomes much more difficult and requires models with sufficient flexibility to account for age-related restructuring of the GRIN medium.

The purpose of this manuscript is to explore the restructuring of the lens GRIN medium with age, and its effect on optical power and spherical aberration (SA). With more advanced

Biomedical Optics EXPRESS

modelling, one could view the effect of GRIN structure on the ageing eye. We use a new model capable of separately showing the effects of the axial and radial GRIN profiles to revisit the lens paradox. To our knowledge, there is no other detailed study on the ageing GRIN lens structure. Our goal is to illustrate that the lens paradox can be resolved, by showing how a restructuring of the GRIN medium can match the power of the ageing eye to a published longitudinal study. We provide a more detailed analysis of changes in the lens and whole eye during the ageing process. In particular, we show how SA of the eye changes suitably with age.

The AVOCADO lens model [2] includes a new description of the lens GRIN bulk, in which an internal iso-indicial contour height is given by:

$$\rho^2 = 2\zeta^{2m+1}R_a(\zeta T_a + z) - \zeta^{2m}(1 + K_a)(\zeta T_a + z)^2 + \zeta^{2m-1}B_a(\zeta T_a + z)^3, \tag{1}$$

where R_a and K_a are the radius and conic constant, and T_a is the thickness from nucleus to pole of the anterior lens portion—these parameters are shown in Fig. 1. The axial and radial GRIN profiles can be decoupled, allowing independent alteration of optical power and SA. This decoupling is an improvement of the previous geometry-invariant GIGL model [3], in which the axial and radial GRIN profiles feature the same steepness (power law exponent, P).

In the AVOCADO model, the aberrations are calculated using exact raytracing, by solving the differential ray equation [4]. To our knowledge, exact raytracing has not been performed in a human lens model in which the surfaces are described by a conicoid plus a higher-order aspheric term. Furthermore, the AVOCADO model can be used to analyse accommodation of the human lens [5], in an analytical way [6]. Figure 1 is a schematic of the lens model, showing the iso-indicial contours. The refractive index of the lens along its optical axis in the z direction is given by:

$$n(\zeta)\Big|_{\rho=0} = n_c + (n_s - n_c)\,\zeta^{2P} \quad \text{along}\, z - \text{axis}, \tag{2}$$

where ζ is the normalised distance from lens centre to external surface; n_s and n_c are the refractive indices at the lens surface and centre, respectively; and P is an age-dependent parameter controlling the slope of the refractive index towards the lens periphery. In the lens radial direction (ρ), perpendicular to the optical axis, the refractive index changes as:

$$n(\zeta)\Big|_{z=0} = n_c + (n_s - n_c)\,\zeta^{\frac{2P}{m+1}} \quad \text{perpendicular to}\, z - \text{axis}. \tag{3}$$

From Eqs. 2 & 3, we can see that the exponents of the axial and radial refractive index profiles are related by the factor $(m + 1)$; which, as shown below, approaches 1 as the lens ages. Interestingly, the radial GRIN profile affects the lens optical power in the paraxial region since the $2P/(m + 1)$ exponent is related to optical power by the scaling of radii of the iso-indicial contours: $r = \zeta^{2m+1}R$, where R is the radius of the external lens surface—see Eq. (1). This offers another interpretation of parameter m, namely that the axial gradient of the curvature $C = 1/R$ of the iso-indicial contours in the lens anterior segment is:

$$\frac{\mathrm{d}C}{\mathrm{d}z} \propto \frac{2m+1}{r\zeta} = \frac{2m+1}{r^{\frac{2m+2}{2m+1}}}.$$

In comparison, a recent study by Navarro and López-Gil considers a GRIN lens with an axial curvature gradient of G/r^2, where G is a constant called the curvature gradient parameter [7]. Similar to G, the axial curvature gradient near the lens surface is proportional to $2m + 1$.

The present paper illustrates how one could use the AVOCADO model to account for the lens paradox, a term coined by Brown and first mentioned in a 1986 paper by Koretz and Handelman [8–10]. Briefly, the lens paradox is the measured decrease (or relatively slow increase) in refractive power of the human eye, despite the fact that the lens radii become more highly curved and hence the surfaces become more powerful. The paradoxical nature arises because,

Biomedical Optics EXPRESS

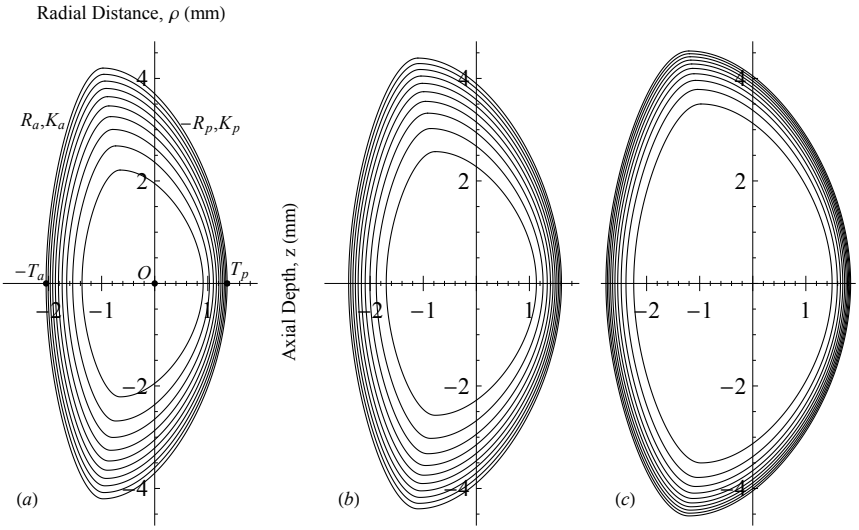

Fig. 1. Iso-indicial contours of lenses modelled at different ages. (a): $age = 20$, $P = 2.87$, $m = 0.60$; (b): $age = 45$, $P = 3.30$, $m = 0.54$; (c): $age = 70$, $P = 5.49$, $m = 0.23$. The "avocado" effect can be seen in (a), while the geometry-invariant shape is seen in (c).

although the lens surfaces become more powerful, the total lens power decreases. While the refractive state of the eye is relatively stable from 20–40 years [11], a hyperopic shift is observed until approximately 60 years [12–18]. After the age of approximately 70 years, some studies found a myopic shift in refraction [13–15, 17], probably due to the formation of cataract [19–21]. This is summarised in Fig. 20.1 of *Optics of the Human Eye*, by Atchison and Smith [22].

2. Method of reconstructing the ageing human eye

In a 2011 paper by Tabernero *et al.* [23], the authors model, amongst other aberrations, the SA of the ageing human eye. For this modelling exercise, the authors chose to use Le Grand's original eye model as initial data for the eye [24]. The lens radii decreased, and central lens thickness increased, at the rates found experimentally by Dubbelman *et al.* [25, 26], which are summarised in Table 1. The equivalent refractive index changed by the amount $\Delta n_{\text{eq}} = -0.00039/\text{yr}$. The change of the cornea with age was assumed to be negligible [27, 28].

To view the age-related change in SA, they performed a series of simulations. The first of these simulations did not incorporate any age-related changes in the lens conic constants. The authors expected to find an increase in SA with age, as reported in the literature. However, they found that SA decreased monotonically, as shown in their Fig. 6(a). This unexpected behaviour was seen as paradoxical and was termed the "spherical aberration paradox". To solve the paradox, they allowed the lens conic constants to increase with age, as found in another study of Dubbelman and van der Heijde [25]:

$$\Delta K_a = +0.03/\text{yr} \quad \text{and} \quad \Delta K_p = +0.07/\text{yr}. \tag{4}$$

With these changes, the simulated SA increased too quickly with age. As a final adjustment, the authors divided the age-related changes in conic constants by 2 and re-simulated the SA. In this case, the SA increased satisfactorily with age, albeit rather slowly than the literature data.

The most obvious explanation for the paradoxical behaviour observed in Tabernero *et al.*'s study is the over-simplified lens model containing a homogeneous refractive index. To study the effect of a GRIN lens structure on the behaviour of ocular SA with age, we performed

Biomedical Optics EXPRESS

our own set of simulations. The simulations employed the AVOCADO lens model with age-dependent parameters P and m. The lens was initially set up in a similar manner to Tabernero's study. Instead of the relatively old Le Grand eye [24], we chose data from the 2014 study of Rafael Navarro [29]. We chose data for the x-meridional section only. Our cornea changes non-negligibly with age, with the anterior radius given by: $Rc_a = 7.85 - 0.0051 \times$ age mm, and posterior: $Rc_p = 6.20$ mm.

The conic constant of the posterior corneal surface (Kc_p) was chosen as above from the work of Navarro. Due to the large refractive index difference at the anterior corneal surface, the anterior corneal conic constant (Kc_a) will have a considerable effect on SA of the eye. Considering the large range of values reported in the literature, Kc_a was rounded to a generic value with one significant figure; its change with age is taken from Navarro, as above. The conic constants therefore change with age according to: $Kc_a(\text{age}) = -0.3 - 0.0009 \times$ age and $Kc_p(\text{age}) = -0.56$.

As stated, the initial ocular data were taken from Navarro's 2014 study [29], but the *lens age-related changes* were the same as that used by Tabernero, taken from the work of Dubbelman and van der Heijde [25]. These are summarised in Table 1, where T_c = corneal thickness, T_{cl} = cornea–lens thickness (anterior chamber depth), T = lens thickness, and T_a and T_p are the anterior and posterior thicknesses of the lens from nucleus to pole. Finally, as with Tabernero's initial simulation, the conic constants of the lens do not change with age—the values are again taken from Navarro's 2014 study and are: $K_a = -4$ and $K_p = -3$.

Table 1. Intraocular distances and lens radii used in modelling the ageing eye.

$T_c = 0.55$	$T_a = 0.6 \times T$; $T_p = 0.4 \times T$
$T_{cl}(\text{age}) = 3.87 - 0.010 \times \text{age}$	$R_a(\text{age}) = 12.7 - 0.057 \times \text{age}$
$T(\text{age}) = 2.93 + 0.024 \times \text{age}$	$R_p(\text{age}) = 5.9 - 0.012 \times \text{age}$

The refractive indices of the cornea, aqueous and vitreous humour were taken from the 2005 paper by Escudero-Sanz and Navarro [30] for the wavelength 589.3 nm. Regarding the lens internal structure, the central and surface refractive indices of the lens were $n_c = 1.415$ and $n_s = 1.37$, respectively [2]. Parameters P and m both affect the GRIN profile in the radial direction according to the exponent $2P/(m+1)$. If the *axial* GRIN profile is governed by the exponent $2P$, then the value $(m+1)$ can be considered as the scaling between the axial and radial GRIN profiles of the lens [2]. When $m = 0$, the axial and radial GRIN profiles are identical, and this results in the geometry-invariant (GIGL) model [3]. The value of P was taken from the 2007 study of Navarro and co-workers [31], so that the value of $2P$ is:

$$2P(\text{age}) = 5.7 + \left(\frac{\text{age}}{46}\right)^4. \tag{5}$$

Interestingly, the normalisation value of 46 years in the denominator above might correspond to the onset of presbyopia in mid-life.

Finally, we chose an age-related dependence for parameter m, which describes the rate of change of iso-indicial contour curvature from surface to centre. As the eye ages, we expect that m tends towards zero, so that the older lens model approaches the GIGL model. For this, we chose the simple dependence:

$$m(\text{age}) = 0.6 - \left(\frac{\text{age}}{90}\right)^4. \tag{6}$$

The constant terms in the above equation ensure that m decreases with age at a sensible rate, with 90 years representing the rather old eye. Note that the expression for m has the same fourth-power

Biomedical Optics EXPRESS

dependence on age as parameter P, and the normalisation value of 90 years might correspond to the age at which the eye undergoes senile degeneration. With these values for P and m, the GRIN axial profile exponent has a value at age zero of $2P = 5.7$, while the radial exponent is $(m + 1) = (0.6 + 1) = 1.6$ times smaller, with a value of 3.6. At approximately 80 years of age, m is reduced from 0.6 to zero, and hence the axial and radial refractive index profile exponents are the same, resulting in geometry-invariant iso-indicial contours (the case described by the GIGL model). At this age, P has a value of 7.4.

3. Results

Regarding the choice of the GRIN structure, P was chosen in accordance with the previously published 2007 study of Navarro and co-workers (Eq. (5)) [31]. The choice of $m = 0.6 - (\text{age}/90)^4$ is such that it produces the "avocado" effect seen in younger lenses, where the peripheral iso-indicial contours are more closely spaced in the axial direction than the radial direction—see Fig. 1. Furthermore, this choice of m stabilises the power of the eye with age. Shown in Fig. 2a is the change in optical power vs age of the simulated eye, calculated using exact raytracing to locate the paraxial focus [2], which is equivalent to the wavefront curvature matching method [32]. Note that conic constants do not affect optical power and so the power is the same for all conic constants. From this figure, we can make two observations. First, directly comparing ages 10 and 70 years, the power of the eye increases relatively little overall; second, the power clearly shows non-monotonic behaviour with age, and has a maximum value at approximately 40 years of age, mainly due to the normalisation in the empirical formula of Eq. 5.

To compare the age-related change in ocular power using the AVOCADO model to the cross-sectional and longitudinal work of Saunders [14, 15] (Fig. 2b), we note that the data in Fig. 2b relate to *refractive error*. That is, the values refer to the correction required to remove defocus in the eye. For example, if an eye is myopic, the image will focus in front of the retina and so a negative corrective lens is required. Hence, ocular power is negatively related to refractive correction.

Using Eq. 6 for m, the resulting refractive error is shown as the orange trace in Fig. 2b. We can see that the refractive correction has a minimum at approximately 40 years of age; this is the first time that modelling has come close to replicating the works of Saunders [14, 15], which show a non-monotonic change in refractive error vs age; these are seen as the dashed green traces in Fig. 2b.

The particular choice of starting values for this eye produced a large amount of negative SA in the eye. Since SA is strongly coupled to conic constants, and conic constants do not affect optical power, this was remedied by simply changing the lens conic constants to more positive (less negative) values of $K_a = -3.0$ and $K_p = -2.5$.

The result of our initial SA simulation is shown as the green plot in Fig. 3. We can see in this example that SA increases with age, but begins to plateau after the age of about 60 years. This simple initial simulation is very promising, as it does not show Tabernero *et al.*'s observed paradoxical behaviour of SA vs age. The reason for the sensible behaviour in this simulation is that the lens contains a GRIN structure.

A survey of the literature shows that there are two main age-related trends in SA. The first is the result of Salmon and van de Pol [33], who found that SA has the polynomial dependence $y = 0.000045 \times \text{age}^2 - 0.002038 \times \text{age} + 0.06408$. Second, the average of studies (excluding Salmon and van de Pol) explicitly showing polynomial (linear or other) fits of SA vs age showed that for a 5 mm pupil SA has a mean value of 0.056 μm at 30 years of age, with a slope of 0.002 μm/yr. These are shown in Fig. 3 as the dashed blue and red traces, respectively. In addition to clarifying the SA paradox, we can adjust the age-related change in lens conic constants to match these summary values of experimentally-observed age-related changes in SA.

Biomedical Optics EXPRESS

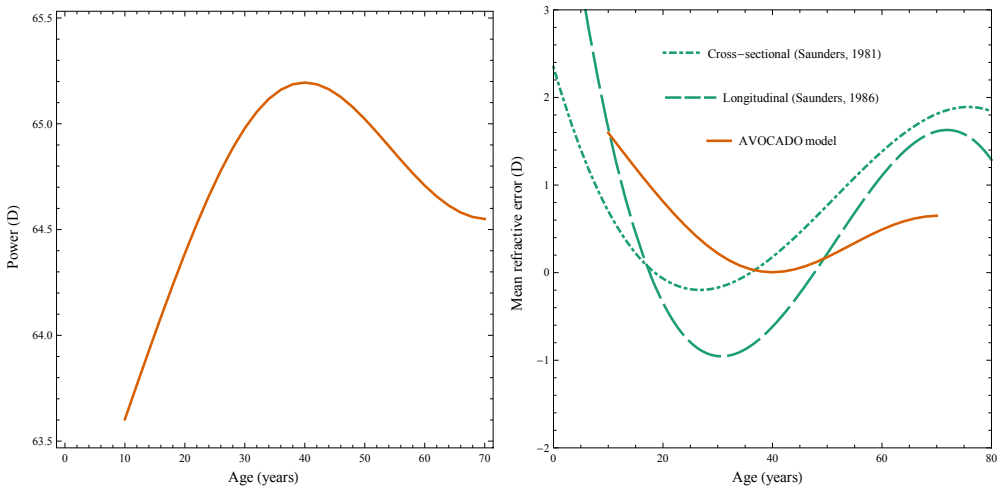

(a) (b)

Fig. 2. Simulation of ocular power (a) and refractive error (b) vs age using the AVOCADO model, with the age-dependence of $m = 0.6 - (\text{age}/90)^4$. Refractive error (b) is compared to the findings of Saunders [14, 15], after [22].

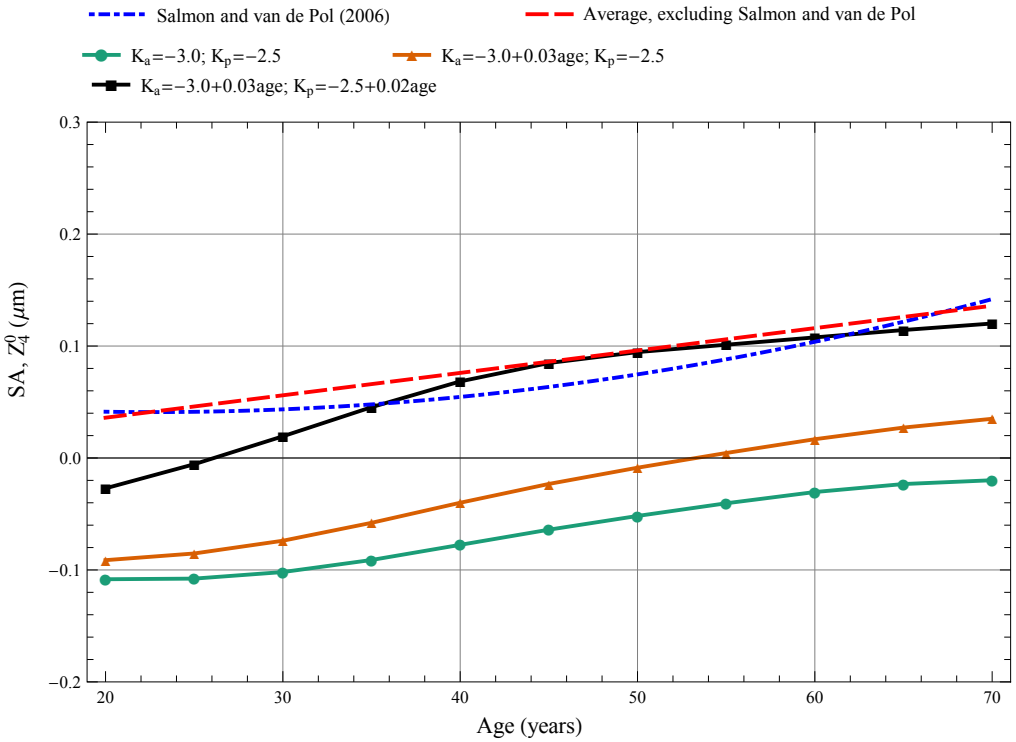

Fig. 3. Simulation of SA vs age with 5 mm pupil diameter, for comparison with the work of Tabernero *et al.* [23].

Biomedical Optics EXPRESS

The conic constants of the lens surfaces are very difficult to measure accurately *in vivo* [6], and hence any age-related changes are not easily recognised. For example, Tabernero *et al.* [23] initially use the age-related changes in conic constants found by Dubbelman and van der Heijde [25]. They argue that the changes were found to be non-significant; hence, they adjusted the lens conic constants vs age to match experimental data on SA from the literature. We follow the same procedure here for the posterior conic, which is more difficult to measure experimentally in the *in vivo* eye. The orange trace in Fig. 3 is the result of changing the anterior lens conic constant by the amount +0.03/yr, in accordance with the findings of Dubbelman and van der Heijde [25]. The black trace is the result when the posterior lens conic is also increased by the amount +0.02/yr. This value of +0.02 was chosen so that the ratio of anterior conic to posterior conic decreases with age at approximately the same rate as the ratio of the anterior radius to posterior radius. As we can see, the black trace compares well with the experimental summary of the preceding paragraph; in particular, the values between the ages of approximately 35 to 65, and the slope agree well with the experimental data (dashed blue and red traces).

Worthy of note is the observation that there are many possible configurations of the lens conic constants that produce the same lenticular SA. While this is a problem for generic modelling, this will not be a problem with future customised modelling where, for example, the lens conic constants could be accurately measured in experiments. While the exact matching of SA vs age with the conics is not well-defined, this does not dilute the valuable finding that the AVOCADO model can explain both the power and SA paradoxes. Furthermore, until now, there has been no physical basis for the introduction of measures to explain the (optical power) lens paradox. For example, the age-related reduction in equivalent refractive index has not been analysed in terms of restructuring of the GRIN medium. The AVOCADO model, containing a physically relevant change in parameter m with age, produces optical power that follows the correct trend; the physical relevance comes from the age-related change in iso-indicial contour shape. As a result, m is useful not only in qualitatively reproducing the features of the ageing eye ("avocado" effect), but also in quantitatively accounting for optical power and hence equivalent refractive index.

Also worthy of note is the age-related increase in lens conic constants required to produce a lens whose SA increases with age. This is opposite to the trend observed in the accommodating eye, where the conics decrease, resulting in an accommodative decrease in SA. Conceptually, this contradicts the observation that the ageing eye is similar to the accommodating eye [34]. While it is true that the central thickness increases and radii decrease in both cases, the processes are similar in this regard only. One particular difference is that the lens diameter decreases with accommodation, whereas it increases with age. The mechanisms of accommodation and ageing are not yet fully understood, but the following could be considered. When the lens accommodates, the zonular forces are reduced and the elastic capsule forms the accommodated lens shape [35]. In this case, the reduction of stretching effort on the capsule allows the lens conics to decrease, resulting in a negative change in SA. On the contrary, the ageing unaccommodated eye grows in volume and so there will be a larger stretching force on the elastic capsule. Perhaps this stretching causes the age-related increase in conic constants and hence SA.

4. Conclusion

A future aim of personalised modelling of the human lens is the creation of a model that is as simple as possible, yet is fully compatible with all aspects of the lens. These include anatomical, biomechanical and optical characteristics. We can see from the literature that there has been a trade-off between anatomical accuracy and simplicity. Traditionally, simpler models of the lens have been used for generating personalised models. The reason that more sophisticated models have not been used is, because, with increasing complexity, the problem might become over-determined; that is, where a model has more degrees of freedom than constraints from

Biomedical Optics EXPRESS

experimental data, it quickly loses relevance, due to the lack of a unique solution.

With increasing model flexibility, more subject-specific personalised models can be created. Personalisation is performed where the geometrical properties of the lens are measured experimentally and are used as input for the model. The lens GRIN can then be optimised to match the experimentally determined refractive power and aberration values. In the current work, the introduction of a single extra parameter m has enabled us to simultaneously predict power and SA, and visualise the "avocado" effect (the experimental observation that the iso-indicial contours of younger lenses show a more rapid increase in curvature as they approach the nucleus). The constraints for m include the qualitative quasi-invariance of power with age and the imitation of the "avocado" effect in younger eyes. These constraints are not strong, but are sufficient for optimising m as a function of age. This has allowed us to explore the lens paradoxes in a model which has additional degrees of freedom. In addition to accounting for the age-related changes in ocular power and iso-indicial contour shape, parameter m was found to produce the correct age-related trend in ocular SA.

In the work of Tabernero and co-workers [23, 36], the use of a constant equivalent refractive index for the lens gave difficulty in matching the theoretical and experimental data. This led to the conclusion that there exists a sort of "spherical aberration paradox" within the human eye.

We have demonstrated that the AVOCADO model is useful for analysing age-related restructuring of the GRIN medium, and is capable of predicting refractive power and SA. This model can be used as a practical tool for matching experimentally measured optical constraints of power and SA with ageing and accommodation, while simultaneously satisfying several mechanical constraints, such as constant volume and continuity of iso-indicial contours.

Funding

The Irish Research Council, application RS/2012/351.

Disclosures

The authors declare that there are no conflicts of interest related to this article.